Tracking unstable steady states and periodic orbits of oscillatory and chaotic electrochemical systems using delayed feedback control

István Z. Kiss
Department of Chemical Engineering, University of Virginia, Charlottesville, Virginia 22904

Zoltán Kazsu and Vilmos Gáspár
Institute of Physical Chemistry, University of Debrecen, P.O. Box 7, Debrecen-4010, Hungary

(Received 14 March 2006; accepted 12 June 2006; published online 31 July 2006)

Experimental results are presented on successful application of delayed-feedback control algorithms for tracking unstable steady states and periodic orbits of electrochemical dissolution systems. Time-delay autosynchronization and delay optimization with a descent gradient method were applied for stationary states and periodic orbits, respectively. These tracking algorithms are utilized in constructing *experimental bifurcation diagrams* of the studied electrochemical systems in which Hopf, saddle-node, saddle-loop, and period-doubling bifurcations take place. © *2006 American Institute of Physics*. [DOI: 10.1063/1.2219702]

Identification of equilibrium and nonequilibrium states as a function of external parameters and exploration of how these states are attained from different initial conditions are fundamental in characterizing the behavior of nonlinear dynamical systems. With these "passive" observations, however, direct information can be obtained from the stable states only. Indirect information on unstable states could be obtained by studying how the stable states are approached and how they are changed upon varying external parameters. With the application of control techniques, however, direct experimental information on unstable states also become attainable. In this paper, we use an efficient control technique, the time delayed feedback, to locate unstable steady states and periodic orbits in electrochemical systems as a control parameter, the circuit potential, is varied. We show how this information can be applied to gain insight into the dynamics of complex chemical reactions.

I. INTRODUCTION

Controlling dynamical systems has been the subject of intense investigations in nonlinear dynamics. Dynamical aspects of control include stabilization of unstable steady states and periodic orbits and creation of complex dynamical behaviors that do not exist without control. Counterintuitively, chaotic systems are excellent choices for control as small perturbations can have profound effects on the dynamics due to large sensitivity to initial conditions.[1–3] Feedback type control methods for stabilizing unstable periodic orbits (UPOs) of chaotic systems are based on classical control theory[4] and usually classified by the character of control perturbations. The extent of perturbations can be calculated discretely in the OGY-based methods ("pole placement")[5] or continuously in the delayed-feedback methods.[6] There are successful implementations in a wide variety of chemical systems for both types of control methodologies; delayed-feedback techniques with trial-and-error control parameters are usually easier to implement[7–11] but the OGY-based techniques provide control formula with explicit control constants.[12–16]

Important goals in nonlinear dynamics are to find the location of stable and unstable steady states and periodic orbits in the bifurcation diagrams and to investigate the properties of these states as some parameters are changed. In numerical studies the problem is formalized in terms of continuation: once a solution of a dynamical system is known for a set of parameters, the solution can be constructed as a function of the parameters. In experiments, the continuation of states are called *tracking*.[17] Once control of an unstable state is attained at a given bifurcation parameter, the problem of tracking involves the correction of constants in the control law so that the control loop always finds the unstable state.[18] Experiments with tracking in physical systems were done with electronic circuits,[19] diode resonators,[20] laser systems,[21,22] driven (bronze[23] or magnetoelastic[24]) ribbons and pendulum.[25] Most of these applications are based on the prediction-correction-type modification of OGY-based chaos control methods.[17]

For chemical and biological systems, however, experiments are lacking probably due to the complex calculations that are required in the tracking procedures. To simplify the procedure, an OGY-method based algorithm, the simple proportional feedback (SPF) can be used for control[14,26] and tracking.[27] In the chaotic Belousov-Zhabotinsky (BZ) reaction,[28] tracking of unstable periodic orbits was carried out as the mean residence time was slowly varied in a continuously-fed stirred tank reactor. General application of this method is troublesome[29] in chemical systems. Although chaotic behavior can be represented by one-dimensional return maps in many chemical systems (e.g., in the BZ reaction,[30] electrochemical systems,[31] *p*H oscillators,[32] combustion reactions,[15] and biochemical systems[33]), the perturbation of a control parameter can increase the dimensionality of the system. Methods do exist to overcome this

problem,[12,29,34] however, the tracking algorithms become complicated again.[28,35]

In this paper, we investigate efficient tracking procedures based on the delayed-feedback control algorithm. We present experimental results on application of the delayed-feedback method[6] for tracking unstable steady states and periodic orbits. Tracking of unstable steady states is carried out in the Ni-sulfuric acid electrochemical system;[36] this system can exhibit various (Hopf, saddle-node, and saddle-loop[36,37]) bifurcations. We use tracking algorithms to construct experimental bifurcation diagrams. Tracking of unstable periodic orbits is carried out in the chaotic copper-phosphoric acid electrochemical system[38] to explore the underlying dynamical features of the chaotic behavior.[14,39]

II. EXPERIMENT

Experiments were performed in a standard three-electrode electrochemical cell equipped with a Radelkis OH-0933P saturated calomel electrode as reference, and a Radelkis OH-9437 Pt-sheet counterelectrode (area 5 cm^2). In the Ni-sulfuric acid (4.5 mol/dm^3) system the working electrode was a Ni wire (99,99%+, Aldrich, diameter 1 mm) embedded in epoxy. In the experiments with copper (99,99%, diameter 5 mm) in phosphoric acid electrolyte (85%, Spektrum-3D) a rod was embedded in epoxy and fit onto a rotating disk. The electrodes were polished with a series of sandpapers. The cell contained 70 cm^3 electrolyte, and was thermostated at −5 °C and 10 °C in the experiments with copper and nickel, respectively, with the Lauda RMB thermostat. The cell was connected to a computer controlled potentiostat (Elektroflex EF451) through a series resistor R. The potential between the working and reference electrodes was set with a resolution of 0.1 and 0.02 mV, respectively, for simple potentiostatic and control experiments. Current was measured with an accuracy of 0.001 mA with the ammeter built in the potentiostat. Sampling frequencies of 200 Hz were applied for data acquisition.

III. DELAYED-FEEDBACK METHODS FOR TRACKING PROCEDURES

The delayed-feedback control technique[6] imposes a perturbation onto a system parameter $\delta V(t)$ proportional to the difference between a state variable, $i(t)$, and its value with a time delay, $i(t-\tau)$,

$$\delta V(t) = K(i(t) - i(t-\tau)), \tag{1}$$

where K is the control gain. It is often possible to stabilize an UPO that has a period of τ with appropriate control gain. When the target dynamics is an unstable steady state τ can be chosen to be a small value close to zero.[11] It was found that the simple feedback given by Eq. (1) is not capable of stabilizing an unstable object with arbitrary eigenvalues (or Floquet exponent).[40]

An extended time-delay autosynchronization (ETDAS) method was proposed[41–45] to circumvent this problem by extending the feedback formula [Eq. (1)] with terms of larger delays,

$$\delta V(t) = K\left[i(t) - (1-r)\sum_{k=1}^{\infty} r^{k-1} i(t-k\tau) \right], \tag{2}$$

where control parameter $-1 \leqslant r < 1$ regulates the weight of information from the past. The limit of $r \to 0$ corresponds to simple delayed feedback; highly unstable orbits can be stabilized with $r \to 1$. We note that $\delta V(t)$ vanishes when an UPO is successfully stabilized since $i(t) = i(t-k\tau)$ for any k.

Tracking of unstable orbits can be achieved by continuously updating K, r, and τ as a response to changes in system parameters that affect the period and stability of the unstable orbits. Among these control parameters, τ is of the greatest importance.[46–48] An analytical approximation of τ was obtained by calculating the frequency of the control signal.[49] We apply an even simpler method by Yu and Chen;[40,50] the algorithm is based on a gradient descent search for an optimized value of τ. An error function $E(t)$ is defined

$$E(t) = \frac{1}{n}\sum_{l=1}^{n} [i(t - l\delta t) - i(t - l\delta t - \tau)]^2, \tag{3}$$

where δt is the data acquisition interval and n is the total number of data used for $E(t)$. The gradient can be obtained as

$$\frac{\partial E(t)}{\partial \tau} = \frac{2}{n}\sum_{l=1}^{n} [i(t - l\delta t) - i(t - l\delta t - \tau)] \frac{\mathrm{d}i(t - l\delta t - \tau)}{\mathrm{d}t}. \tag{4}$$

The period can be adjusted by

$$\tau_{m+1} = \tau_m - \beta \frac{\partial E(t)}{\partial \tau}, \tag{5}$$

where β determines the convergence rate. Note that the adjustment of τ is not required for tracking unstable steady states (USS) since in this case an appropriate, small constant value can be applied.[11,51]

IV. TRACKING UNSTABLE STEADY STATES IN OSCILLATORY ELECTRODISSOLUTION OF NICKEL

Potentiostatic electrodissolution of nickel exhibits oscillations and bistability depending on experimental conditions such as circuit potential (V), external resistance (R), concentration of the electrolyte (c), etc.[52] This system was classified as an electrochemical oscillator with a Hidden-Negative-Differential Resistance (H-NDR).[53] Our goal is to track the unstable steady states resulting from a supercritical Hopf bifurcation and explore the important dynamical features of the system as a function of V at various values of R.

Tracking of USSs by the delayed-feedback technique requires proper choice of K and τ or K,τ, and r in Eq. (1) or Eq. (2), respectively. Oscillatory electrodissolution of Ni in sulfuric acid can be controlled with both simple time-delay feedback [Eq. (1)] and ETDAS [Eq. (2)] methods. Successful control experiments are shown in Fig. 1; the EDTAS method [Fig. 1(b)] provides a more robust way for control; the target state is reached in a shorter period and the perturbations are smaller. We note that after control was turned off the system always returned to the oscillatory state and thus no hysteresis was observed in these experiments.

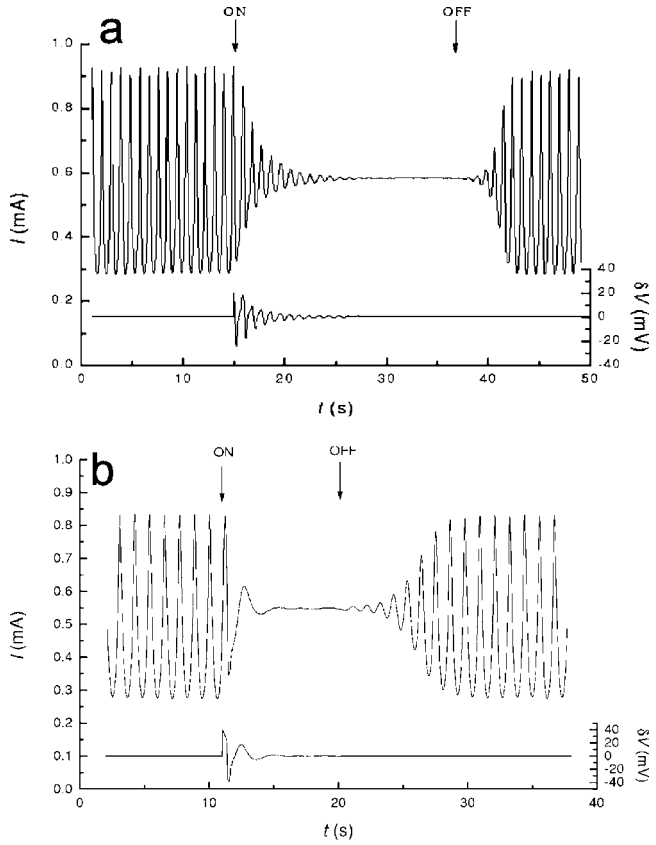

FIG. 1. Stabilizing steady state in oscillatory electrodissolution of Ni in sulfuric acid. (a) Simple delayed-feedback algorithm [$K=40$ mV/mA, $\tau=0.3$ s in Eq. (1)]. (b) Extended delayed-feedback algorithm [in Eq. (2) $K=187$ mV/mA, $\tau=0.15$ s, $r=0.7$, and the maximum value of k is 9]. Current (left axis) and potential perturbation (right axis) vs time for an interval when the control was switched on and off. $V=1.590$ V, $R=200\ \Omega$.

Both methods were tested for tracking unstable steady states; in these experiments, control is attempted with slow linear variation of the circuit potential V at four different external resistances in the range of $100\ \Omega \leqslant R \leqslant 300\ \Omega$. For tracking, the simple delayed feedback method was found to perform poorly; it failed to stabilize the unstable steady states at large circuit potentials and resistance values. Bifurcation diagrams obtained with the ETDAS method are presented in Fig. 2. The "traditional" bifurcation diagrams (showing stable behavior with upward and downward scans) are overlayed with the position of the tracked unstable steady state. Independent impedance analysis was carried out *without* an external resistance connected to the cell. This analysis is capable of predicting Hopf and saddle-node bifurcation points at different R by measuring the impedance characteristics of the cell[54–56] at $R \to 0$; the predicted bifurcations points are also shown.

At $R=150\ \Omega$ [Fig. 2(a)] the steady state is unstable between $V=1560$ mV and $V=1650$ mV. However, using the tracking algorithm, the unstable steady state can be stabilized in this region. Impedance analysis indicates that the stability losses are through Hopf bifurcations. The current drops to a low value at $V=1750$ mV. The impedance analysis confirmed that the upper steady state is destroyed through a saddle-node bifurcation at this potential. During the backward scan of V the low-current (passive) state was always found to be stable until another saddle-node bifurcation at $V=1660$ mV. We also *estimated* the position of the saddle by connecting the two saddle-node bifurcation points [dashed line in Fig. 2(a)]. Our attempts to track the saddle-point with EDTAS—in accordance with a theoretical proof[57]—were unsuccessful; approximate locations of these saddle states were recently confirmed with an adaptive controller.[58]

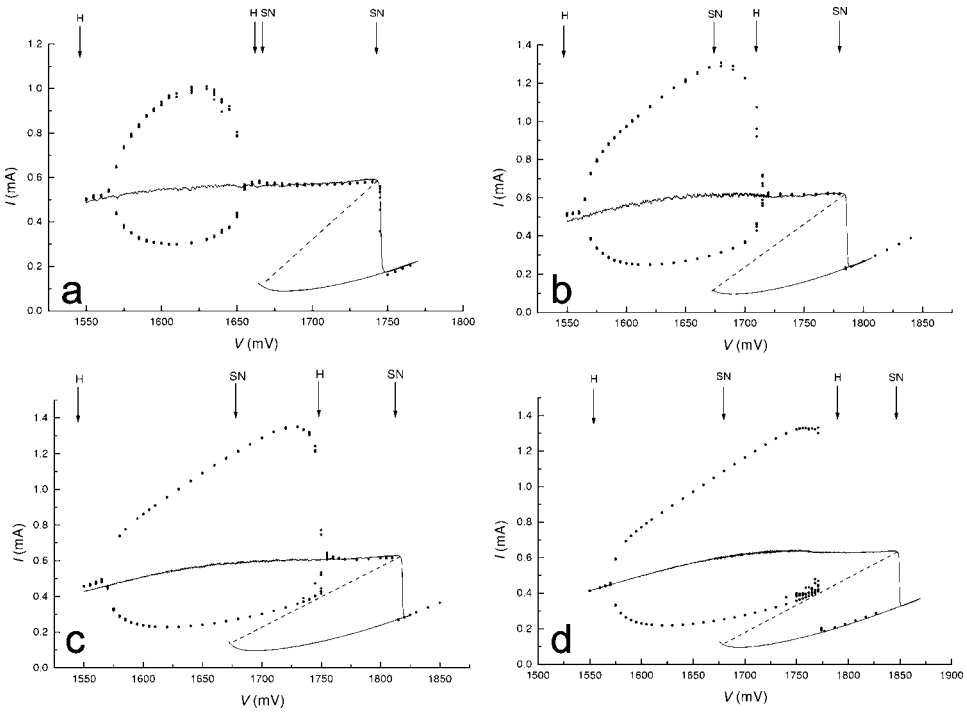

FIG. 2. Experimental bifurcation diagrams of the Ni-sulfuric acid electrodissolution system showing the minima and the maxima of the current oscillations (solid circles) and the steady states stabilized by the extended delayed-feedback tracking algorithm (line) vs circuit potential at different external resistors. (a) $R=150\ \Omega$; (b) $R=200\ \Omega$; (c) $R=250\ \Omega$; (d) $R=300\ \Omega$. The H and SN symbols denote the Hopf and saddle-node bifurcation points predicted by impedance spectroscopy. Dashed line represents the estimated position of the saddle points assuming a "traditional" Z-shaped bifurcation diagram. The scanning rate of the potential variation was 1 mV/s. Control parameters in Eq. (2): $\tau=0.15$ s, $r=0.7$, and $K=163$ mV/mA in panel (a) and $K=187$mV/mA in panels (b)–(d).

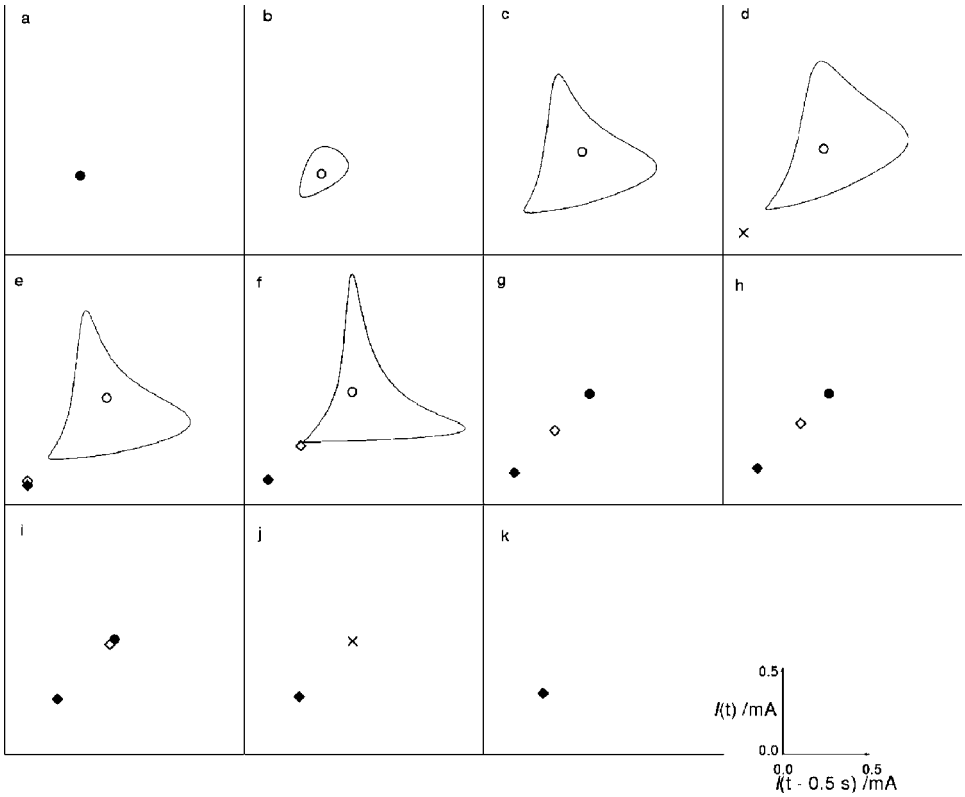

FIG. 3. Reconstructed phase space of the Ni-sulfuric acid system at $R=300\ \Omega$ [corresponding to Fig. 2(d)] obtained at various circuit potentials: (a) 1.565 V; (b) 1.575 V; (c) 1.660 V; (d) 1.676 V; (e) 1.680 V; (f) 1.746 V; (g) 1.774 V; (h) 1.788 V; (i) 1.841 V; (j) 1.848 V; (k) 1.856 V. Solid (hollow) circles: upper stable (unstable) steady states. The solid and open diamonds represent the stable lower and the unstable saddle points, respectively. ×: saddle-node points; solid curve: limit-cycle oscillations.

At a somewhat larger resistance, $R=200\ \Omega$ [Fig. 2(b)], the bifurcation diagram shows that oscillations have larger amplitudes; at about $V=1710$ mV the limit cycle and the predicted position of the saddle point approach each other. At $R=250\ \Omega$ [Fig. 2(c)] these tendencies continue; finally, at $R=300\ \Omega$, the limit cycle and the saddle point coincides, and oscillations cease abruptly at $V=1775$ mV [Fig. 2(d)]. The homoclinic nature of the bifurcation is further evidenced by the linear variation of the period as a function of the logarithmic distance from the bifurcation point.[37] Right before the saddle-loop bifurcation the minima of oscillations are rather scattered implying that complex dynamics may arise due to homoclinic chaos. In several experiments chaotic-like temporal variation of the current was observed, however, the reproducibility was rather poor. [By further increasing the resistance ($R=350\ \Omega$) this complex dynamic was not observed; with $R>300\ \Omega$, however, the EDTAS algorithm failed to control the system with control parameters similar to those at lower resistances.] With the tracking procedure it is possible to stabilize the upper steady state above the homoclinic bifurcation. [Above the upper Hopf bifurcation point ($V=1780$ mV) the steady state is stable and the control algorithm could be turned off.] This upper steady state is destroyed at a relatively large potential ($V=1850$ mV) with a saddle-node bifurcation ($V=1850$ mV).

The observed bifurcation scenarios can be better represented in reconstructed phase-space diagrams (Fig. 3) at $R=300\ \Omega$. By increasing the potential the upper steady state [Fig. 3(a)] loses its stability and a stable limit-cycle appears around the unstable focus [Fig. 3(b)]; the size of the limit cycle increases with increasing potential [Fig. 3(c)]. A saddle-node bifurcation occurs in the low current region at about $V=1.676$ V [Fig. 3(d)]; above this potential the saddle point slowly approaches the limit cycle [Figs. 3(e) and 3(f)]. After the collision of the saddle and the limit cycle [$V=1.774$ V, Fig. 3(g)] the saddle point approaches the upper steady state that is now stable [Fig. 3(h)]. After the collision of the saddle and the node at a $V=1.841$ V [Fig. 3(i)] only the lower steady state can be observed in Fig. 3(j).

V. TRACKING UNSTABLE PERIODIC ORBITS IN CHAOTIC COPPER ELECTRODISSOLUTION

Anodic electrodissolution of copper in phosphoric acid electrolyte exhibits chaotic current oscillations.[59] We use this experimental system to test the efficiency of the tracking procedure with time-delayed feedback control.

A successful control of period-1 unstable orbit is shown in Fig. 4(a) using delayed feedback control. Before control perturbation is switched on ($t<30$ s) the system exhibits low-dimensional chaotic current oscillations.[14] After control is turned on [i.e., the circuit potential is perturbed according to Eq. (1)], periodic oscillations are observed. The control constant τ was chosen to be the approximate period of oscillations ($\tau=0.85$ s) while the control gain K was adjusted to achieve optimal performance. The control is very robust; there is no need to apply ETDAS. However, the control perturbations do not vanish completely. Similar nonvanishing perturbations were also seen in other experimental reports.[9,11] Theoretical analysis proved[49] that such nonvanishing, periodic perturbations are due to the incorrect values of the control parameters K and τ. The asymmetric nature of the oscillating feedback signal is likely due to the asymmetric waveform of the oscillating current. The power spectrum

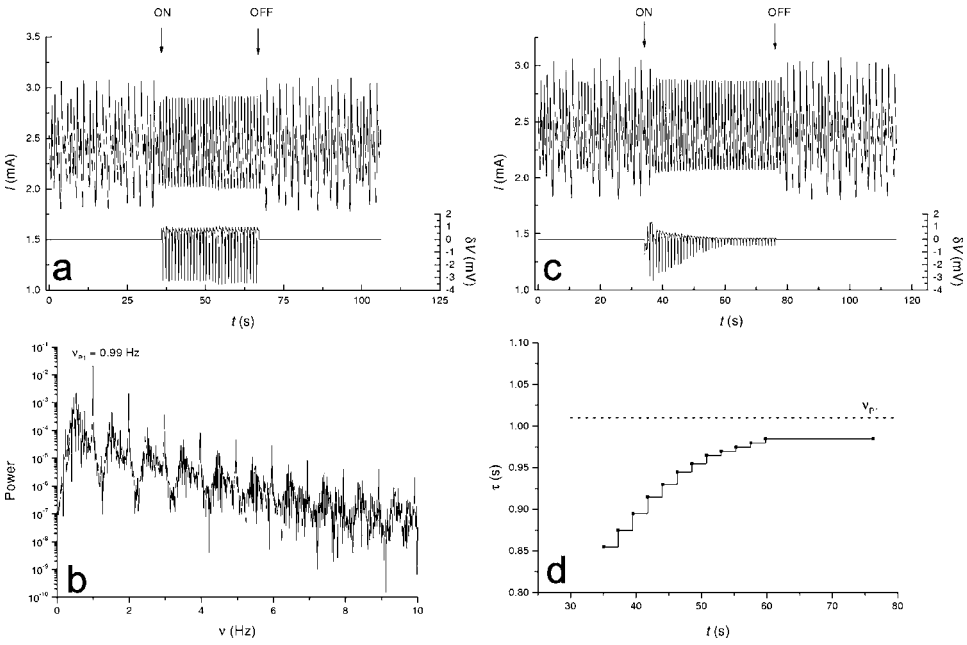

FIG. 4. Controlling chaotic electrodissolution of Cu in phosphoric acid solution. (a) The time series of the current (left axis) and the potential perturbations (right axis). Delayed-feedback technique with $K=4$ mV/mA and $\tau=0.850$ s in Eq. (1) is applied between the arrows. (b) Power spectrum of a time series of chaotic current oscillations. The frequency of the period-1 orbit can be estimated from the strong peak at $\nu_{P1}=0.99$ Hz. (c) Stabilizing the unstable period-1 orbit using the delayed-feedback algorithm [Eq. (1) $K=4$ mV/mA] with corrections to the period, τ [Eq. (5), $\beta=5$ and $n=400$]. The time series of the current (top, left axis) and the potential perturbations (top, right axis) as the period τ is adjusted every 2 s. (d) The adjusted period τ as a function of time. The initial estimate of the period was $\tau=0.85$ s, the same value as used in panel (a). The horizontal dashed line (bottom) represents the period of the unstable orbit estimated from the Fourier spectrum [panel (b)]. Rotation rate: 1540 rpm, $V=557$ mV, and $R=69$ Ω.

of the chaotic oscillations (from independent experiments) is shown in Fig. 4(b); the spectrum exhibits a maximum at $\nu_{P1}=0.990$ Hz; occurrence of peaks in power spectrum is characteristic of phase coherent chaotic behavior and can be considered as an approximation of the frequency of unstable periodic orbits.

The value of the control constant τ can be optimized by using the gradient descent method. After successful control is achieved, the error gradient is evaluated using Eq. (4) and an improvement of τ is automatically calculated with Eq. (5). Stepwise improvements of τ at about every two oscillatory periods during a control procedure are shown in Figs. 4(c) and 4(d). As τ increases to a limiting value of 0.980 s [Fig. 4(c)], the size of control perturbations decrease [Fig. 4(d)]. Control becomes more robust as well since stabilized oscillations show less variations in the amplitude. These experimental results suggest that the gradient descent method dramatically improves control performance by auto-

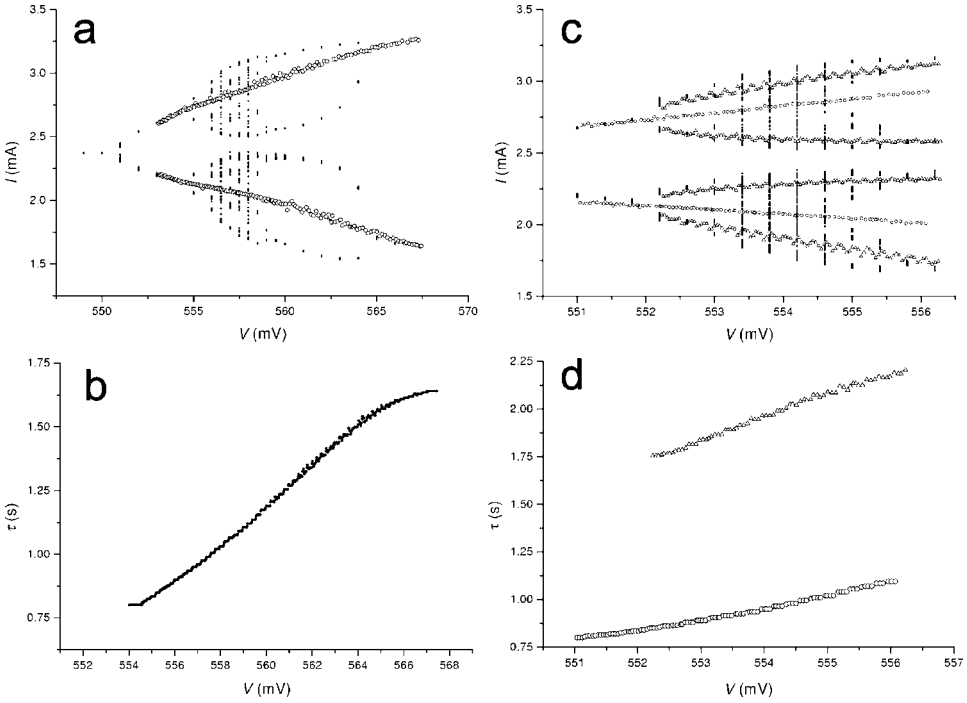

FIG. 5. Tracking unstable period-1 and period-2 orbits in chaotic Cu dissolution in phosphoric acid. (a) Bifurcation diagram showing the maxima and minima of the stable (solid circle) and tracked unstable period-1 (open circle) oscillations. (b) The period of the stabilized orbit obtained using the iterative algorithm [Eq. (5)] with $K=4$ mV/mA, $\beta=5$, $n=400$ [in Eqs. (1) and (5)]. Rotation rate: 1530 rpm, $R=70$ Ω. (c) Bifurcation diagram showing the maxima and minima of the stable (solid circle), tracked unstable period-1 (open circle), and the unstable period-2 (open triangle) oscillations. (d) The period of the stabilized orbits vs circuit potential. For tracking period-1 orbits: $K=4$ mv/mA, $\beta=5$, $n=200$; for period-2: $K=3$mV/mA, $\beta=5$, $n=200$. Rotation rate: 1500 rpm, $R=69$ Ω. The scan rate of the circuit potential during the tracking is 0.02 mV/s.

matically setting the value of the control constant τ.

The gradient descent method requires a trial-and-error procedure to adjust the convergence rate β. If the convergence rate is too small the procedure cannot follow fast changes of τ. Conversely, if the convergence rate is too large, the iteration may result in overshooting the period of the unstable periodic orbit, and occasionally, no convergence could be reached. Since reliable evaluation of the error function requires at least one oscillation ($\approx$200 data points in our setup) we typically used 200–400 data points (about 1–2 cycles) for calculation of the gradient with a convergence rate of $\beta=5$.

Without switching the control on, steady-state—period-1 — period-2 — period-4 — chaos — period-4 — period-2 — period-1 bifurcation structure can be observed as the potential is varied in the bifurcation diagram in Fig. 5(a). Using the delayed feedback control with autosetting time delay, the unstable period-1 orbit can be traced through a period doubling cascade. The determined period, shown in Fig. 5(b), strongly depends on the bifurcation parameter, the circuit potential; it increases from about 0.8 to 1.7 s. Note that the period-1 orbit was successfully traced in the entire bifurcation diagram covering the stability loss of the period-1 orbit.

Similar experiments were carried out to track both the unstable period-2 and period-1 orbits in consecutive experiments. Figure 5(c) shows the maxima and minima of current oscillations of the uncontrolled system, the tracked period-1, and period-2 orbits. In these experiments a relatively small range of circuit potential is investigated that spans mainly over the chaotic region. The period of the unstable period-2 orbit (τ_{P2}) shown in Fig. 5(d) is always greater than twice the period of the period-1 orbit (τ_{P1}). Obviously, if (τ_{P2}) were nearly equal to ($2\tau_{P1}$) for some V, the tracking would be extremely difficult exposing a limitation on the applicability of algorithm.

VI. DISCUSSION

Traditional experimental studies of nonlinear systems typically relies on observation of stable dynamical behaviors. In low-dimensional systems, limited information on the possible bifurcations can be obtained by analyzing the properties of stable behavior, for example, observing changes in period and amplitude of oscillations as the bifurcation point is approached. However, visualization of unstable states and identification of bifurcation carries valuable information that is typically obtained in models numerically or theoretically.

We applied the delayed feedback tracking algorithm for stabilizing unstable steady states in the nickel electrodissolution system. Complementary impedance spectroscopy was applied to identify local bifurcation points of steady states. The combination of the two approaches enabled us to construct an experimental bifurcation diagram for Ni electrodissolution in the parameter space of the circuit potential and external resistance. We successfully identified the local Hopf and saddle-node bifurcation points; visualization of limit cycles and a (predicted) position of the saddle point showed a global homoclinic (saddle-loop) bifurcation.

Unstable period-1 and period-2 orbits were tracked through a period-doubling cascade during the electrodissolution of Cu in phosphoric acid electrolyte. The applied method is much simpler than the SPF method applied earlier.[28] It does not require complex calculations, it is easy to implement, and the application of delayed-feedback control techniques provide a robust control. As a result of simplicity, the method neither requires nor provides the Floquet exponent of the unstable orbit. On the other hand, when the value of the exponent is required for an application, either the SPF-based (or more generally OGY-based) tracking algorithm should be preferred or the method must be extended with an eigenvalue calculator module.[60–62]

Construction of bifurcation diagrams, done by the tracking method proposed in this paper, can aid the classification and categorization[63–65] of oscillatory systems. In homogeneous oscillatory chemical reactions, for example, bifurcation diagrams were found to be useful for exploring skeletal reaction mechanism, the connectivity of reaction networks, and the role of essential species.[66]

From a technological point of view, states that possess economically favorable properties could be attained with tracking. The stability region of a multimode laser was extended with the tracking algorithm.[22] In the nickel dissolution system studied here, the high current (large chemical reaction rate) state could be stabilized in a potential region where, without control, the electrode would be passive. The stable parts of the bifurcation diagrams obtained with nickel electrodissolution exhibit many similarities to those of formic acid electro-oxidation on platinum electrode.[67] It is likely that the unstable stationary states with large currents exist (similar to the nickel system) at large overpotentials in formic acid oxidation; the inhibition of the electrocatalytic surface due to CO adsorption could be overcome with the proposed tracking algorithm. The simplicity and robustness of the tracking method tested here could thus find applications in many other nonlinear dynamical systems for the purpose of construction of experimental bifurcation diagrams and tracing unstable states of fundamental or technological importance.

ACKNOWLEDGMENT

We acknowledge OTKA T038071 for financial support.

[1] B. R. Andrievskii and A. L. Fradkov, Autom. Remote Control (Engl. Transl.) **64**, 673 (2003).
[2] B. R. Andrievskii and A. L. Fradkov, Autom. Remote Control (Engl. Transl.) **65**, 505 (2004).
[3] *Focus Issue on: Control and Synchronization of Chaos*, edited by W. L. Ditto and K. Showalter (AIP, New York, 1997), Vol. 7.
[4] G. Stephanopoulos, *Chemical Process Control: An Introduction to Theory and Practice* (Prentice-Hall, Englewood Cliffs, 1983).
[5] E. Ott, C. Grebogi, and J. A. Yorke, Phys. Rev. Lett. **64**, 1196 (1990).
[6] K. Pyragas, Phys. Lett. A **170**, 421 (1992).
[7] A. Lekebusch, A. Förster, and F. W. Schneider, J. Phys. Chem. **99**, 681 (1995).
[8] F. W. Schneider, R. Blittersdorf, A. Förster, T. Hauck, D. Lebender, and J. Müller, J. Phys. Chem. **97**, 12244 (1993).
[9] I. Z. Kiss, V. Gáspár, and J. L. Hudson, J. Phys. Chem. B **104**, 7554 (2000).
[10] X. L. Li, D. Y. Lu, J. B. He, and H. L. Wang, Acta Phys.-Chim. Sin. **18**, 218 (2002).

[11]P. Parmananda, R. Madrigal, M. Rivera, L. Nyikos, I. Z. Kiss, and V. Gáspár, Phys. Rev. E **59**, 5266 (1999).
[12]V. Petrov, V. Gáspár, J. Masere, and K. Showalter, Nature (London) **361**, 240 (1993).
[13]P. Parmananda, P. Sherard, R. W. Rollins, and H. D. Dewald, Phys. Rev. E **47**, R3003 (1993).
[14]I. Z. Kiss, V. Gáspár, L. Nyikos, and P. Parmananda, J. Phys. Chem. A **101**, 8668 (1997).
[15]M. L. Davies, P. A. Halford-Maw, J. Hill, M. R. Tinsley, B. R. Johnson, S. K. Scott, I. Z. Kiss, and V. Gáspár, J. Phys. Chem. A **104**, 9944 (2000).
[16]H. Song, Y. N. Li, L. Chen, Z. S. Cai, Y. J. Li, Z. Hou, and X. Z. Zhao, Phys. Chem. Chem. Phys. **1**, 813 (1999).
[17]I. B. Schwartz and I. Triandaf, Phys. Rev. A **46**, 7439 (1992).
[18]I. B. Schwartz, T. W. Carr, and I. Triandaf, Chaos **7**, 664 (1997).
[19]T. L. Carrol, I. Triandaf, I. B. Schwartz, and L. Pecora, Phys. Rev. A **46**, 6189 (1992).
[20]J. C. Shin, S. I. Kwun, and Y. Kim, Int. J. Bifurcation Chaos Appl. Sci. Eng. **6**, 769 (1996).
[21]E. Bielawski, D. Derozier, and P. Glorieux, Phys. Rev. E **49**, R971 (1994).
[22]Z. Gills, C. Iwata, R. Roy, I. B. Schwartz, and I. Triandaf, Phys. Rev. Lett. **69**, 3169 (1992).
[23]U. Dressler, T. Ritz, A. S. Z. Schweinsberg, R. Doerner, B. Hübinger, and W. Martienssen, Phys. Rev. E **51**, 1845 (1995).
[24]V. In, W. L. Ditto, and M. L. Spano, Phys. Rev. E **51**, R2689 (1995).
[25]R. Doerner, B. Hübinger, and W. Martienssen, Int. J. Bifurcation Chaos Appl. Sci. Eng. **5**, 1175 (1995).
[26]B. Peng, V. Petrov, and K. Showalter, J. Phys. Chem. **95**, 4957 (1991).
[27]V. Petrov, M. Crowley, and K. Showalter, Int. J. Bifurcation Chaos Appl. Sci. Eng. **4**, 1311 (1994a).
[28]V. Petrov, M. Crowley, and K. Showalter, Phys. Rev. Lett. **72**, 2955 (1994b).
[29]V. Petrov, B. Peng, and K. Showalter, J. Chem. Phys. **96**, 7506 (1992).
[30]J. L. Hudson and J. C. Mankin, J. Chem. Phys. **74**, 6171 (1981).
[31]J. L. Hudson and T. T. Tsotsis, Chem. Eng. Sci. **49**, 1493 (1994).
[32]G. Rábai and I. Hanazaki, J. Phys. Chem. **100**, 15454 (1996).
[33]L. F. Olsen and H. Degn, Nature (London) **267**, 177 (1977).
[34]R. W. Rollins, P. Parmananda, and P. Sherard, Phys. Rev. E **47**, R780 (1993).
[35]M. A. Rhode, R. W. Rollins, and H. D. Dewald, Chaos **7**, 653 (1997).
[36]O. Lev, A. Wolffberg, M. Sheintuch, and L. M. Pismen, Chem. Eng. Sci. **43**, 1339 (1988).
[37]M. T. M. Koper, J. Chem. Soc., Faraday Trans. **94**, 1369 (1998).
[38]F. N. Albahadily and M. Schell, J. Chem. Phys. **88**, 4312 (1988).
[39]M. Schell and F. N. Albahadily, J. Chem. Phys. **90**, 822 (1989).
[40]K. Pyragas and T. Tamasevicius, Phys. Lett. A **180**, 99 (1993).
[41]J. E. S. Socolar, D. W. Sukow, and D. J. Gauthier, Phys. Rev. E **50**, 3245 (1994).
[42]C. Beta and A. S. Mikhailov, Physica D **199**, 173 (2004).
[43]J. Schlesner, A. Amann, N. B. Janson, W. Just, and E. Scholl, Phys. Rev. E **68**, 066208 (2003).
[44]J. W. Ryu, W. H. Kye, S. Y. Lee, M. W. Kim, M. Choi, S. Rim, Y. J. Park, and C. M. Kim, Phys. Rev. E **70**, 036220 (2004).
[45]J. Unkelbach, A. Amann, W. Just, and E. Scholl, Phys. Rev. E **68**, 026204 (2003).
[46]A. G. Balanov, N. B. Janson, and E. Scholl, Phys. Rev. E **71**, 016222 (2005).
[47]W. Just, H. Benner, and C. von Loewenich, Physica D **199**, 33 (2004).
[48]O. Morgul, Phys. Lett. A **314**, 278 (2003).
[49]W. Just, T. Bernard, M. Ostheimer, E. Reibold, and H. Benner, Phys. Rev. Lett. **78**, 203 (1997).
[50]X. Yu, in Proceedings of the IEEE International Conference on Decision and Control, San Diego, CA, 1997, pp. 401–405.
[51]P. Parmananda, Phys. Rev. E **67**, 045202 (2003).
[52]O. Lev, A. Wolffberg, L. M. Pismen, and M. Sheintuch, J. Phys. Chem. **93**, 1661 (1989).
[53]M. T. M. Koper, Adv. Chem. Phys. **92**, 161 (1996a).
[54]R. de Levie, J. Electroanal. Chem. Interfacial Electrochem. **25**, 257 (1970).
[55]M. T. M. Koper, J. Electroanal. Chem. **409**, 175 (1996b).
[56]I. Z. Kiss, V. Gáspár, and L. Nyikos, J. Phys. Chem. A **102**, 99 (1998).
[57]H. Nakajima, Phys. Lett. A **232**, 207 (1997).
[58]K. Pyragas, V. Pyragas, I. Z. Kiss, and J. L. Hudson, Phys. Rev. Lett. **89**, 244103 (2002).
[59]C. Letellier, L. Le Sceller, P. Dutertre, G. Gouesbet, Z. Fei, and J. L. Hudson, J. Phys. Chem. **99**, 7016 (1995).
[60]E. Mihaliuk, H. Skodt, F. Hynne, P. G. Sorensen, and K. Showalter, J. Phys. Chem. A **103**, 8246 (1999).
[61]J. S. Anderson, S. Y. Shvartsman, G. Flätgen, I. G. Kevrekidis, R. Rico-Martinez, and K. Krischer, Phys. Rev. Lett. **82**, 532 (1999).
[62]K. Pyragas, Phys. Rev. E **66**, 026207 (2002).
[63]K. Krischer, in *Modern Aspects of Electrochemistry*, edited by B. E. Conway, O. M. Bockris, and R. E. White (Kluwer Academic/Plenum, New York, 1999), Vol. 32, p. 1.
[64]P. Strasser, M. Eiswirth, and M. T. M. Koper, J. Electroanal. Chem. **478**, 50 (1999).
[65]I. Z. Kiss, Z. Kazsu, and V. Gáspár, J. Phys. Chem. A **109**, 9521 (2005).
[66]I. Schreiber and J. Ross, J. Phys. Chem. A **107**, 9846 (2003).
[67]P. Strasser, M. Lübke, F. Raspel, M. Eiswirth, and G. Ertl, J. Chem. Phys. **107**, 979 (1997).